Modelling of the thermo-chemical evolution of Ceres

Wladimir Neumann, Doris Breuer, Tilman Spohn
Deutsches Zentrum für Luft- und Raumfahrt

Abstract number 2055

Introduction

Fig. 1. Artist's impression of Ceres.

Ceres is the largest body in the asteroid belt. It can be seen as one of the remaining examples of the intermediate stages of planetary accretion, which in addition is substantially different from most asteroids. Studies of protoplanetary objects like Ceres and Vesta provide insight into the history of the formation of Earth and other rocky planets. One of Ceres' remarkable properties is its low bulk density of 2077±36 kg m^{-3} [1]. For a nearly chondritic composition, this value indicates either a high average porosity[2], or the presence of a low density phase[3,4]. Numerical modelling[3,4] suggests that this low density phase (water ice or hydrated silicates) differentiated from the silicates forming an icy mantle over a rocky core. However, Ceres' shape and the moment of inertia allow for both a porous and a differentiated structure. In the first case, Ceres would be just a large version of a common asteroid. In the second case, however, this body could exhibit properties characteristic for a planet rather than an asteroid: presence of a core, mantle and crust, as well as a liquid ocean in the past and maybe still a thin basal ocean today.

Parameters

Table 1. Composition, mass and volume fractions of the constituents, and further key parameters for the modelling of compaction (mostly from [7]).

Mineral	Mass fraction	Volume fraction	ρ_{solid}	E	k
	%	%	kg m^{-3}	kJ mol^{-1}	W m^{-1} K^{-1}
serpentine	49.2	46.98	2576	88	$(0.404+0.000246T)^{-1}$
montmorillonite	17.0	17.60	2376	113	0.75
epsomite	7.0	10.25	1680	272	0.4
mirabilite	4.5	7.05	1570	126	0.6
pyrene	3.1	6.00	1270	105	0.27
halite	4.2	4.99	2070	113	$5.4(300.0/T)^{1.14}$
magnetite	15.0	7.13	5175	188	$4.23-1.37\cdot10^{-3}T$
CI-chondrite	**100**	**100**	**2460**	-	-

Table 2: Parameter values used to simulate the radioactive heat production by the short- and long-lived isotopes.

Isotope	Element mass fraction	Isotopic abundance	Half-life a	Decay energy per atom J	Initial heat production W kg^{-1}
^{26}Al	$7.60\cdot10^{-03}$	$5.00\cdot10^{-5}$	$7.17\cdot10^{05}$	6.4154E-13	2.3718900735
^{60}Fe	$1.86\cdot10^{-01}$	$1.60\cdot10^{-6}$	$2.61\cdot10^{06}$	4.8700E-13	0.1683221510
^{53}Mn	$2.18\cdot10^{-03}$	$4.00\cdot10^{-5}$	$3.74\cdot10^{06}$	9.5613E-14	0.0076254432
^{40}K	$6.08\cdot10^{-04}$	$1.5\cdot10^{-3}$	$1.25\cdot10^{09}$	1.1102E-13	0.0008471866
^{232}Th	$2.95\cdot10^{-08}$	1.00	$1.41\cdot10^{10}$	6.4721E-12	0.0000244459
^{235}U	$1.00\cdot10^{-08}$	$7.10\cdot10^{-3}$	$7.04\cdot10^{08}$	7.1129E-12	0.0000012743
^{238}U	$1.00\cdot10^{-08}$	$9.93\cdot10^{-1}$	$4.47\cdot10^{09}$	7.6095E-12	0.0000296491

Dimensions
Present radius of ≈ 470 km is assumed to correspond to ϕ=0.1. From this the reference radius of 454 km of a zero-porosity body is computed. The initial radius of 563 km follows from the reference radius and the initial porosity of 0.4764.

Plastic flow
The creep activation energy E is increased stepwise according to the volume fractions and the activation energies of single minerals during compaction.

Conclusions

- high effective stress and low activation energies enable almost complete compaction of Ceres even for late formation times
- in all simulations the present average porosity falls far below 10% yielding a far higher average density that the measured one
- this argues against the porous structure suggested by [2]
- it is rather unlikely that the low density of Ceres can be explained by a partially porous structure
- thus, Ceres is most probably ice-rich and may have a rocky core and an ice mantle (thus, processes associated with the presence of water need to be considered)
- a more systematic study of the compaction of Ceres similar to that of asteroid Lutetia[8] is necessary in order to exclude the possibility that Ceres is not differentiated and porous completely

Model

For the investigation of the possibility of Ceres being porous we adopted the numerical model from [5] Neumann et al. (2012) which computes the thermal and structural evolution of planetesimals, including compaction of the initially porous primordial material.

$$\rho c_p \frac{\partial T}{\partial t} = \frac{1}{r^2}\frac{\partial}{\partial r}\left(kr^2\frac{\partial T}{\partial r}\right)+Q(r,t) \qquad T(r,t_0)=T_n \qquad \frac{\partial T}{\partial r}\Big|_{r=0}=0$$

$$\frac{\partial T}{\partial r}\Big|_{r=R_p(t)} = \frac{e\sigma_{SB}}{k(R_p(t))}\left(T(t,R_p(t))^4 - T_n^4\right)$$

Porosity-dependent parameters, e. g.:

$$k = k_b\left(e^{-4\phi/\phi_1}+e^{-4.4-4\phi/\phi_2}\right)^{1/4}$$

Radius change due to compaction:

$$R_p(t) = \left(\frac{1-\bar{\phi}(t)}{1-\phi_0}\right)^{1/3}\bar{R}$$

Dynamical scaling of radial variable:

$$\eta = \frac{r}{R_p(t)},\ t \geq t_0$$

Plastic flow steady-state strain rate:

$$\frac{d\varepsilon}{dt} = \frac{1}{D}\frac{dD}{dt} = \frac{\partial \log(1-\phi)}{dt} = C(T)\sigma_1^n$$

Effective stress

$$\sigma_1 = \sigma_0\alpha_1^{-1}\left(D^{2/3}\beta_1^{2/3}R^2-1\right)^{-1}$$

Temperature dependence:

$$C(T) = Bb^{-3}\exp\left(-\frac{E}{GT}\right)$$

ϕ	local porosity
$\bar{\phi}(t)$	average porosity
ϕ_0	initial porosity
$\bar{R}$	reference radius
D	relative density
σ_0	pressure
$n \approx 3/2$	material constant
$\alpha_1 = \pi/4$	geometric constant
$\beta_1 = 8$	geometric constant
$B = 4\cdot10^{-5}$	material constant
$b = 1\mu m$	grain size
E	activation energy
G	gas constant

Fig. 2. Deformation geometry of the simple cubic packing of spherical grains adopted in the present study. **a** Geometry at the contact area between two grains. **b** Simple cubic unit cell. **c** Top view of the simple cubic unit cell. Figure from [6].

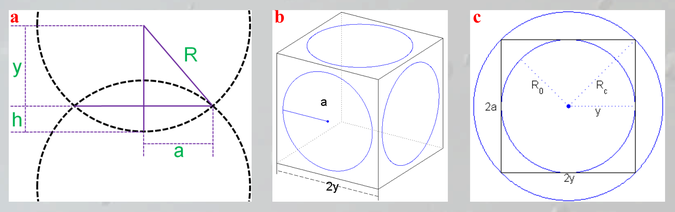

$$\left(\frac{a}{R}\right)^2 = 1-\left(\frac{R_0}{R}\right)^2\left(\frac{1-\phi_0}{1-\phi}\right)^{2/3}$$

$$R = \left[\alpha\left(2+\left(\frac{a}{R}\right)^2\right)\left(1-\left(\frac{a}{R}\right)^2\right)^{1/2}-\beta\right]^{-1/3}$$

Parameters of the simple cubic packing:

Coordination number	6
Initial porosity	0.4764
Critical porosity	0.0349
Geometric constant α	2 π
Geometric constant β	8 π/3
Geometric grain radius	R
Geometric initial grain radius R_0	$(3/4\pi)^{1/3}$
Geometric critical grain radius R_c	0.7155

Results

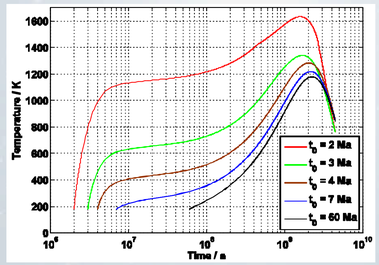

Fig. 3 Central temperature vs. time for different formation times t_0 between 2 and 60 Ma after the CAIs. For small t_0, thermal evolution is dominated by the decay of ^{26}Al, ^{60}Fe and ^{53}Mn with rather high temperatures. For later formation times the slower temperature increase is due to the heating by ^{40}K, ^{232}Th, ^{235}U and ^{238}U. Formation prior to 4 Ma rel. to CAIs indicates silicate-metal differentiation.

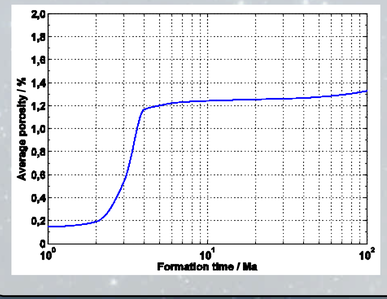

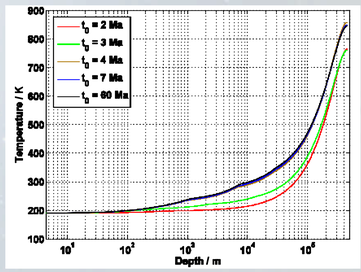

Fig. 4. Temperature profiles taken at 4.5 Ga for varying t_0. Depending on t_0, the temperature of 273 K is reached in the depth of 6-50 km. This supports the existence of liquid water in the sub-surface and interior of the present-day Ceres.

Fig. 7. Present average porosity predicted for different formation times of Ceres. Instantaneous accretion is used as an approximation of the continuous runaway accretion. However, the accreting material in the form of smaller planetesimals could be already pre-heated and pre-compacted. This could have increased the effectiveness of compaction of the early Ceres. Thus, the final average porosities in our calculations serve possibly as an overestimate of the actual one.

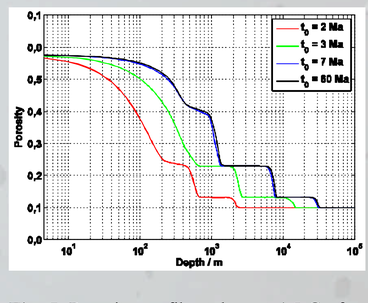

Fig. 5. Porosity profiles taken at 4.5 Ga for varying t_0. The thickness of the porous layer is at best ≈ 30 km. Late formation implies stronger insulation of the interior by a thicker porous layer. However, the final average porosity is < 0.02 in all cases.

Fig. 8. Temporal evolution of the radial distribution of the temperature in the interior of Ceres. Instantaneous accretion is used as an approximation of the continuous runaway accretion. Parallel to the porosity loss, the body shrinks to the final radius of ≈ 456 km. Relatively low activation energies of the minerals (cp. Table 1) enable compaction at the temperatures below ≈ 500 K. Thus, the interior consolidates mostly before the hydrated minerals start to dehydrate.

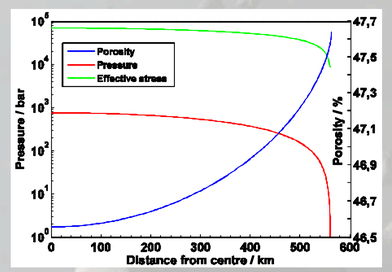

Fig. 6. Samples of the lithostatic pressure, the effective pressure and the corresponding porosity profile. Shows are the profiles assuming t_0 = 7 Ma rel. To CAIs at the time instance t = 8.15 Ma rel. to CAIs. While the porosity deviates only moderately from the initial one, the effective stress lies two orders of magnitude above the lithostatic pressure. With decreasing porosity the lines will converge.

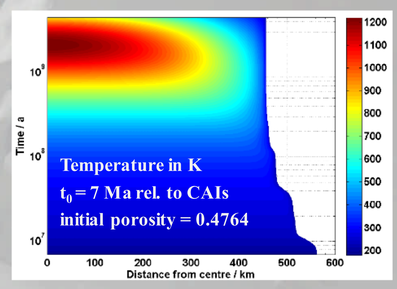

Future Perspectives

Next steps

- **combined treatment of accretion, compaction and differentiation into a rocky core and a water mantle of small icy bodies**
- **consideration of processes like amorphous to crystalline ice transition, ice melting, water-rock differentiation, hydrothermal convection, hydration of silicate minerals (e.g. formation of serpentine from forsterite and H_2O), water release due to dehydration, metal-silicate differentiation, etc.**
- **investigation of most likely evolution scenarios and structural end-members of Ceres depending on its composition and formation time**
- **a better understanding of other bodies like icy asteroids and satellites**
- **conclusions on the astrobiological potential and habitability of Ceres**

Fig. 9. Processes that occur at certain temperatures or temperature ranges in icy planetesimals. Absolute values vary with the assumed composition. The processes influence the temperature and the structure. During the cooling of the body, energy will be released by crystallization of melt and some of the volume changes will be reversed.

Figure from [9]

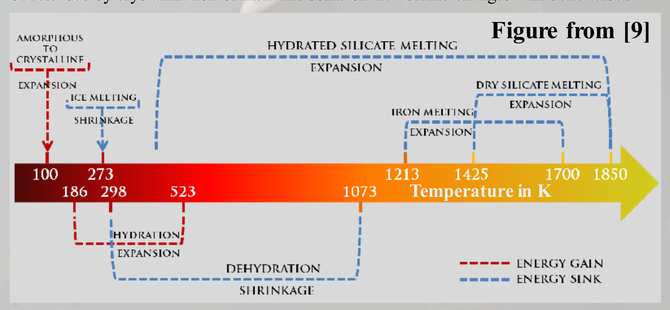

References

[1] Thomas, C., et al., 2005. Differentiation of the asteroid Ceres as revealed by its shape. Nature 437, 224-226.
[2] Zolotov, M. Yu., 2009. On the composition and differentiation of Ceres. Icarus 204, 183-193.
[3] McCord, T. B., Sotin, C., 2005. Ceres: Evolution and current state. JGR 110, E05009 .
[4] Castillo-Rogez, J. C., McCord, T. B. 2010. Ceres' evolution and present state constrained by shape data. Icarus 205, 443-459.
[5] Neumann, W., et al., 2012. Differentiation and core formation in accreting planetesimals. A&A 543, A141.
[6] Neumann, W., et al., 2014. On the modelling of compaction in planetesimals. A&A, in review.
[7] Castillo-Rogez, J. C., 2011. Ceres - Neither a porous, nor salty ball. Icarus, 215, 599-602.
[8] Neumann, W., et al., 2013. The thermo-chemical evolution of asteroid 21 Lutetia. Icarus 224, 126-143.
[9] Neumann, W., et al., 2013. Thermo-chemical evolution of ice-silicate bodies: Application to Ceres. Joint meeting "Paneth Kolloquium", "The first 10 million years of the solar system" (DFG SPP 1385), 21.-23. Okt. 2013, Nördlingen, Germany.

45th LPSC Lunar and Planetary Science Conference
March 17–21, 2014
The Woodlands, Texas
#LPSC2014
The First 10 Million Years of the Solar System – a Planetary Materials Approach – SPP 1385 DFG
Deutsche Forschungsgemeinschaft DFG
Helmholtz Alliance Planetary Evolution and Life
WWU
DLR